

# SCIENTIFIC REPORTS



OPEN

## CL316,243, a $\beta_3$ -adrenergic receptor agonist, induces muscle hypertrophy and increased strength

Daniela Puzzo<sup>1,\*</sup>, Roberto Raiteri<sup>2,\*</sup>, Clotilde Castaldo<sup>3</sup>, Raffaele Capasso<sup>4</sup>, Ester Pagano<sup>4</sup>, Mariateresa Tedesco<sup>2</sup>, Walter Gulisano<sup>1</sup>, Lisaveta Drozd<sup>2</sup>, Pellegrino Lippiello<sup>4</sup>, Agostino Palmeri<sup>1</sup>, Pietro Scotto<sup>4</sup> & Maria Concetta Miniaci<sup>4</sup>

Received: 18 July 2016

Accepted: 28 October 2016

Published: 22 November 2016

Studies *in vitro* have demonstrated that  $\beta_3$ -adrenergic receptors ( $\beta_3$ -ARs) regulate protein metabolism in skeletal muscle by promoting protein synthesis and inhibiting protein degradation. In this study, we evaluated whether activation of  $\beta_3$ -ARs by the selective agonist CL316,243 modifies the functional and structural properties of skeletal muscles of healthy mice. Daily injections of CL316,243 for 15 days resulted in a significant improvement in muscle force production, assessed by grip strength and weight tests, and an increased myofiber cross-sectional area, indicative of muscle hypertrophy. In addition, atomic force microscopy revealed a significant effect of CL316,243 on the transversal stiffness of isolated muscle fibers. Interestingly, the expression level of mammalian target of rapamycin (mTOR) downstream targets and neuronal nitric oxide synthase (NOS) was also found to be enhanced in tibialis anterior and soleus muscles of CL316,243 treated mice, in accordance with previous data linking  $\beta_3$ -ARs to mTOR and NOS signaling pathways. In conclusion, our data suggest that CL316,243 systemic administration might be a novel therapeutic strategy worthy of further investigations in conditions of muscle wasting and weakness associated with aging and muscular diseases.

Studies in humans and animal models have revealed that  $\beta$ -adrenergic receptors ( $\beta$ -ARs) stimulation exerts potent anabolic effects on striated muscles<sup>1,2</sup>. Since activation of  $\beta$ -ARs induces skeletal muscle growth associated, in some cases, with an increase of contractile function<sup>3,4</sup>,  $\beta$ -AR agonists have been proposed as a therapeutic intervention to counteract muscle wasting correlated with aging or chronic diseases such as muscle dystrophy<sup>5-7</sup>. However, the potential for targeting  $\beta$ -ARs in dystrophies has been diminished because of the mild improvements in skeletal mass/function and adverse cardiac events induced by  $\beta_1/\beta_2$  ARs agonists<sup>2</sup>. So far, much of our knowledge on the role of  $\beta$ -AR signaling in skeletal muscle is based on studies focused on  $\beta_2$ -AR agonists, since  $\beta_2$ -AR is considered the predominant subtype in skeletal muscle<sup>2</sup>. However,  $\beta_3$ -ARs have been also identified in human and rodent skeletal muscles<sup>8,9</sup>. Selective activation of  $\beta_3$ -ARs has been established to determine important metabolic responses in skeletal muscle such as glucose uptake, phosphorylation, and oxidation leading to an increase of energy expenditure<sup>10</sup>. In addition,  $\beta_3$ -AR agonists have been shown to affect muscle thermogenesis by increasing the expression of the uncoupling protein-3 (UCP-3), a protein that uncouples mitochondrial respiration from ATP production, thereby dissipating energy in the form of heat<sup>11</sup>. Even though metabolic effects of  $\beta_3$ -AR activation are highly recognized, less is known about the impact of  $\beta_3$ -ARs in the regulation of skeletal muscle structure and function. Using a  $\beta_3$ -AR selective agonist, CL316,243, we have recently demonstrated *in vitro* that  $\beta_3$ -ARs play a critical role in the regulation of protein metabolism in skeletal muscle<sup>12</sup>. In particular, we found that CL316,243 induced a significant increase of skeletal muscle constitutive proteins into muscle cell proteins such as myosin heavy chain, myosin light chain, and actin in rat L6 myocytes. Such anabolic effect was associated with the activation of PI3K/Akt/mTOR pathway, via Gi/o protein, resulting in an increase

<sup>1</sup>Department of Biomedical and Biotechnological Sciences - Section of Physiology, University of Catania, Catania, Italy. <sup>2</sup>Department of Informatics, Bioengineering, Robotics, and System Engineering, University of Genova, Italy. <sup>3</sup>Department of Public Health, School of Medicine and Surgery, University of Naples Federico II, Naples, Italy. <sup>4</sup>Department of Pharmacy, University of Naples Federico II, Naples, Italy. \*These authors contributed equally to this work. Correspondence and requests for materials should be addressed to M.C.M. (email: maria.miniaci@unina.it)

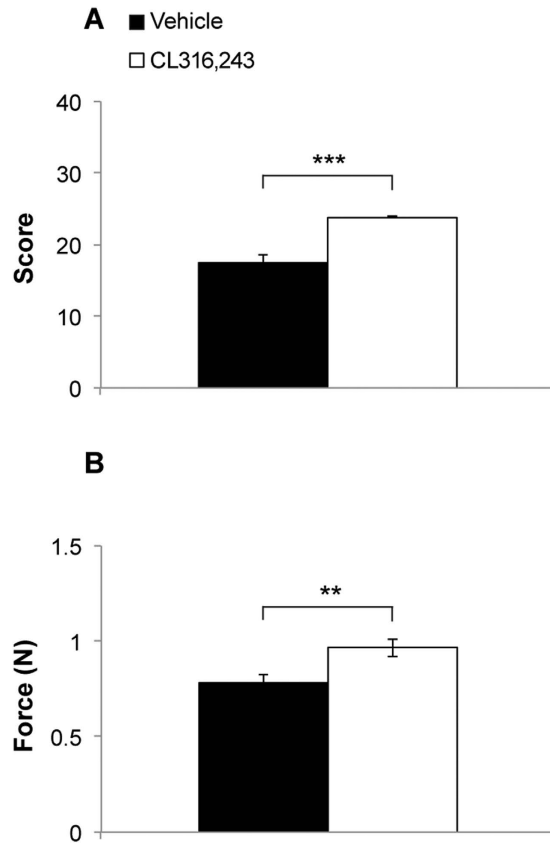


**Figure 1. Effects of treatment with CL316,243 on muscular strength in wild type mice.** (A) Mice treated with the  $\beta_3$ -AR agonist CL316,243 show an increase in the strength score. The score was calculated as the product of the number of links in the heaviest chain held for the full 3 sec, multiplied by the time (sec) it was held (n = 10 CL316,243-treated mice vs n = 9 vehicle-treated mice, unpaired t-test:  $t_{(17)} = 5.495$ ,  $p < 0.0001$ ). (B) Grip test shows an increase in peak force in CL316,243-treated mice compared to vehicle (n = 10/9; unpaired t-test:  $t_{(17)} = 2.978$ ,  $p = 0.008$ ). \*\*\* $p < 0.0001$ , \*\* $p < 0.01$ .

of p70S6 kinase (p70<sup>S6K</sup>) and protein translation. Another signaling pathway that has been linked to  $\beta_3$ -AR is the G protein inhibitory (Gi)-nitric oxide (NO) pathway<sup>13</sup>. In ventricular muscles, activation of the  $\beta_3$ -AR receptors by BRL 37344 is accompanied by decreased contractility via NO production. The  $\beta_3$ -AR-induced negative inotropic effect was shown to be inhibited by the NOS inhibitor L-NAME and could be reversed by an excess of the NOS-substrate, L-arginine<sup>14</sup>.

Based on these lines of evidence, we first examined whether the *in vivo* administration of the  $\beta_3$ -AR agonist CL316,243 affected skeletal muscle strength in adult mice. By using atomic force microscopy (AFM), we next determined whether  $\beta_3$ -AR stimulation modifies the mechanical properties of dissociated skeletal muscle fibers. Furthermore, to gain more insight into the molecular mechanism underlying the  $\beta_3$ -AR function in skeletal muscle, we investigated whether CL316,243 treatment was associated with an upregulation of the putative  $\beta_3$ -AR signaling transduction pathways, involving p70<sup>S6K</sup> as well as the neuronal nitric oxide synthase (nNOS), which is considered the main source of NO in skeletal muscle<sup>15</sup>.

## Results

### CL316,243 treatment induces an increase in skeletal muscle strength in adult healthy mice.

Muscular strength was assessed in wild-type healthy mice treated with the selective  $\beta_3$ -ARs agonist CL316,243 (CL; 1 mg/kg) or saline once per day for 15 days. As shown in Fig. 1A, CL-treated mice exhibited a significant increase in the strength score on the weight test ( $23.9 \pm 0.1$  vs.  $17.44 \pm 1.23$ ;  $p < 0.0001$ ). These results were confirmed by the grip strength test, showing that CL316,243 treatment resulted in a 23% increase of peak force with respect to control ( $0.96 \pm 0.04$  vs.  $0.78 \pm 0.03$ ;  $p = 0.008$ ; Fig. 1B). Furthermore, we found that injections of CL316,243 at this dose and duration did not affect mice body weight (corresponding to  $27.81 \pm 0.31$  grams before CL-treatment vs.  $27.93 \pm 0.30$  grams after CL-treatment;  $t_{(17)} = 0.275$ ,  $p = 0.787$ ).

**CL316,243 regulates the mechanical properties of skeletal muscle fibers.** To determine whether  $\beta_3$ -AR activation can also affect the mechanical properties of the cytoskeleton, we measured the transversal stiffness of CL316,243-treated flexor digitorum brevis (FDB) fibers in the relaxed state by means of AFM-based nanoindentation technique. AFM is a useful tool for studying cell mechanics since it allows to apply controlled loads in the nanoNewtown range to living cells and measure the corresponding cell deformation with nanometer

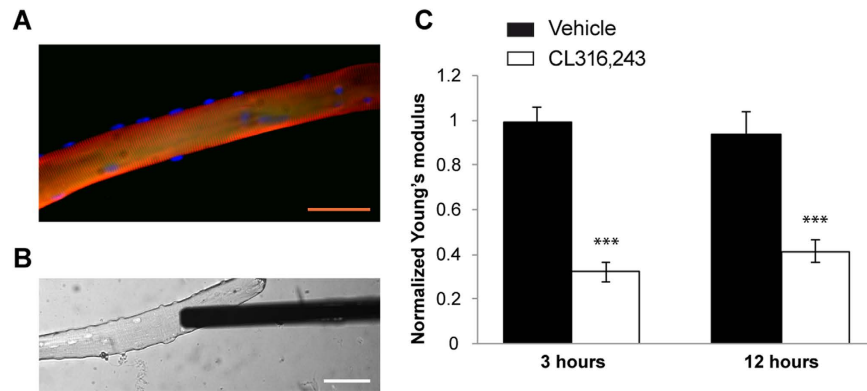


**Figure 2. Effects of CL316,243 treatment on muscle stiffness.** (A) Immunofluorescence image of a dissociated FDB muscle fiber to visualize Z-bands (red), F-actin (green) and nuclei (blue). (B) Bright field image of a single FDB fiber and the AFM rectangular cantilever during nanoindentation measurements. (C) Normalized stiffness indicated as Young's modulus, was obtained by AFM nanoindentation measurements from single dissociated muscle fibers, at 200 nm penetration depth. Fibers were incubated with CL316,243 or vehicle and stiffness was measured after 3 or 12 h treatment ( $n = 4-5$  fibers/treatment, two-way ANOVA for treatment  $F_{(1,14)} = 81.022$ ,  $p < 0.0001$ , time  $F_{(1,14)} = 0.087$ ;  $p = 0.772$ , and treatment x time interaction  $F_{(1,14)} = 1.218$ ;  $p = 0.288$ ). \*\*\* $p < 0.0001$ . Calibration bar = 100  $\mu\text{m}$ .

resolution<sup>16-18</sup> (Fig. 2A and B). AFM measurements were performed on single dissociated muscle fibers incubated with either control solution or 1  $\mu\text{M}$  CL316,243 for 3 or 12 hours. As shown in Fig. 2C, treatment with CL316,243 induced a significant reduction of transversal stiffness in the sub-sarcolemma region, at an indentation depth of 200 nm, when compared to untreated fibers at both time points ( $p < 0.0001$ ).

#### CL316,243 treatment induces an increase in muscle fiber cross-sectional area in adult healthy mice.

To assess whether the increase in muscle strength induced by CL316,243 was associated with muscle hypertrophy, we measured the cross-sectional area (CSA) of hindlimb of CL-treated mice. For this purpose, we selected the soleus and the tibialis anterior (TA), as representative of slow-twitch and fast-twitch muscles, respectively. Morphometric analysis of muscle fibers revealed that CL316,243 induced a significant increase by 83% in TA muscle fiber CSA ( $p < 0.0001$ ), whereas in soleus CSA was slightly increased by 11% ( $p = 0.13$ ) compared to control (Fig. 3A and B). The examined muscles did not show any sign of degeneration such as intracytoplasmic vacuoles and centralized nuclei.

#### CL316,243 treatment increases the skeletal muscle expression level of p70<sup>S6K</sup> and rpS6.

According to our previous studies *in vitro*,  $\beta_3$ -ARs stimulation up-regulates protein synthesis in myocyte cultures and this effect is likely mediated by the PI3K- mTOR- p70<sup>S6K</sup> signaling pathway activation. Indeed, the CL316,243-induced increase of p70<sup>S6K</sup> was markedly inhibited by wortmannin, a PI3K inhibitor, and rapamycin, a specific inhibitor of mTOR<sup>12</sup>. Based on these observations, we examined whether the *in vivo* administration of CL316,243 modulates the expression of p70<sup>S6K</sup> and its downstream target, rpS6, in skeletal muscles obtained from mice treated with CL316,243 or vehicle. As shown in Fig. 4A and B, western blot analysis revealed that the expression level of phospho-p70<sup>S6K</sup> was significantly higher in both TA and soleus muscles of CL316,243-treated mice with respect to vehicle-treated mice ( $p < 0.0001$ ). This up-regulation of p70<sup>S6K</sup> was associated with an increased expression of phospho-rpS6 in TA ( $p < 0.0001$ ) and soleus ( $p < 0.05$ ) when compared to control conditions (Fig. 4A and C).

#### CL316,243 treatment increases the skeletal muscle expression level of neuronal-NOS.

Studies in murine myocardium have demonstrated that application of the  $\beta_3$ -AR agonist, BRL 37344, modulates NOS activity and increases NO formation<sup>19</sup>. Additional evidence for nNOS coupling to  $\beta_3$ -AR comes from studies showing that the  $\beta_3$ -AR-induced negative inotropic effect is absent in cardiomyocytes of nNOS-deficient (NOS1<sup>-/-</sup>) mice as well as in control cardiomyocytes with acute nNOS inhibition<sup>20</sup>. We, therefore, examined whether CL316,243 treatment *in vivo* affected the expression level of nNOS, which is the most abundant NOS isoform in skeletal muscle. As shown in Fig. 5A and B, nNOS appeared to be regulated in both TA ( $p < 0.01$ ) and soleus ( $p < 0.0001$ ) of CL316,243-treated mice with respect to vehicle-treated mice. These data suggest that nNOS may be involved in the  $\beta_3$ -AR effects on skeletal muscle.

## Discussion

This study provides the first demonstration that  $\beta_3$ -AR activation has important anabolic effects on skeletal muscle. In particular, we show that CL316,243 treatment induces a significant increase of muscle CSA and strength in adult healthy mice compared to controls. The increase in CSA, indicative of muscle hypertrophy, was particularly evident in TA compared to soleus muscle, suggesting a difference in response to  $\beta_3$ -agonists between fast- and slow-twitch skeletal muscles. The increase of CSA in TA, a muscle containing a high quantity of fast-contracting fibers, is in agreement with several studies reporting a hypertrophic effect of  $\beta_2$ -AR agonist mainly in fast-twitch

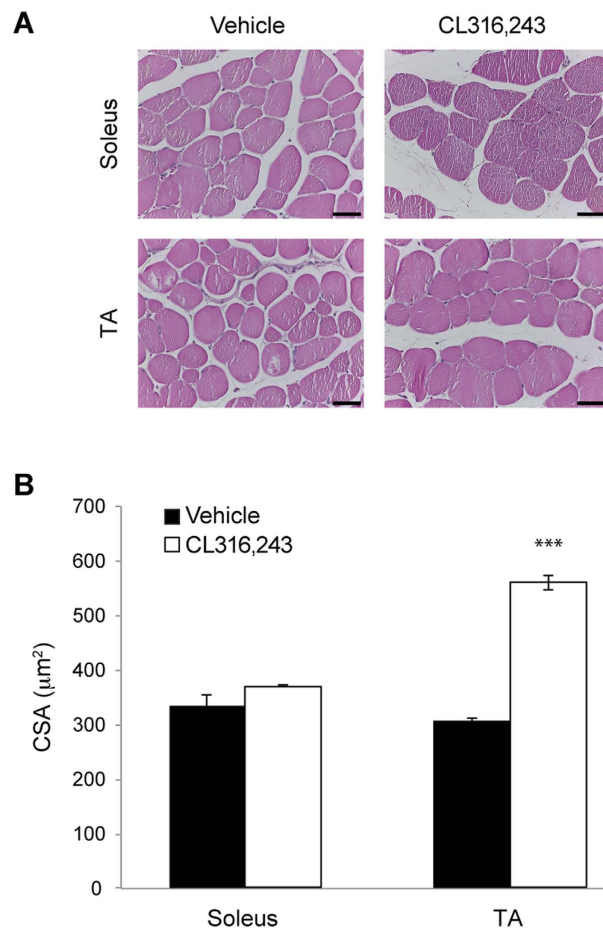


**Figure 3. Effects of CL316,243 treatment on fiber cross-sectional area.** (A) Representative images of hematoxylin and eosin staining of soleus (upper panels) and TA (bottom panels) muscles from mice treated with CL316,243 or vehicle. The stained muscle sections were analyzed for CSA. (B) Bar Graph showing the increase in TA CSA after treatment with CL316,243 compared to vehicle (TA CSA,  $n = 3-4$  samples/treatment; unpaired  $t$ -test:  $t_{(5)} = 15.08$ ,  $p < 0.0001$ ; soleus CSA  $n = 3$  soleus muscle samples/treatment; unpaired  $t$ -test:  $t_{(4)} = 1.86$ ;  $p = 0.13$ ). \*\*\* $p < 0.0001$ . Calibration bar =  $20 \mu\text{m}$ .

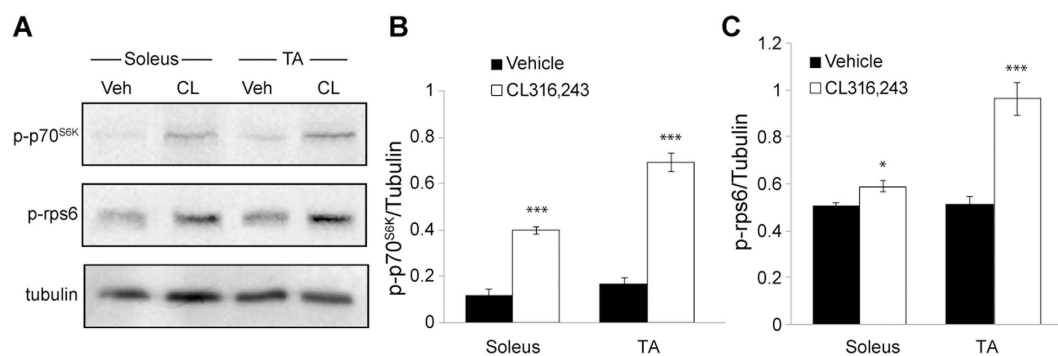


**Figure 4. Effects of CL316,243 treatment on phospho-p70<sup>S6K</sup> and phospho-rpS6 expression levels in skeletal muscles.** (A) Representative western blot showing the p-p70<sup>S6K</sup> and p-rpS6 protein expression in TA and soleus skeletal muscles of mice treated with CL316,243 (CL) or vehicle (Veh).  $\alpha$ -Tubulin was used as internal loading control. (B) Densitometric quantification of protein shows significant increase of p-p70<sup>S6K</sup> in both soleus and TA after treatment with CL316,243 ( $n = 5/5$ ; for soleus unpaired  $t$ -test:  $t_{(8)} = 8.51$ ,  $p < 0.0001$ ; for TA unpaired  $t$ -test:  $t_{(8)} = 6.04$ ,  $p < 0.0001$ ). (C) Densitometric analysis shows significant increase of p-rpS6 p70<sup>S6K</sup> in both soleus and TA after treatment with CL316,243 ( $n = 5/5$ ; for soleus unpaired  $t$ -test:  $t_{(8)} = 2.93$ ,  $p = 0.019$ ; for TA unpaired  $t$ -test:  $t_{(8)} = 5.91$ ,  $p < 0.0001$ ). \* $p < 0.05$ , \*\*\* $p < 0.0001$ .

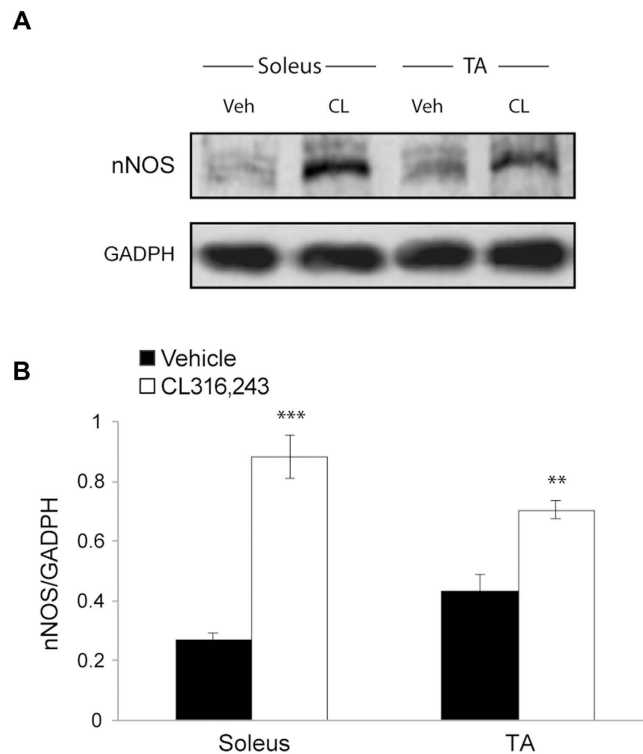


**Figure 5. Effects of CL316,243 treatment on nNOS expression levels in skeletal muscles.** (A) Representative western blot showing the nNOS protein expression in TA and soleus skeletal muscles of mice treated with CL316,243 (CL) or vehicle (Veh). GADPH was used as internal loading control. (B) Densitometric quantification of protein shows significant increase of nNOS in both soleus and TA after treatment with CL316,243 ( $n = 5/5$ ; for soleus unpaired t-test:  $t_{(8)} = 8.41$ ,  $p < 0.0001$ ; for TA unpaired t-test:  $t_{(8)} = 4.57$ ,  $p = 0.002$ ). \*\* $p < 0.01$ , \*\*\* $p < 0.0001$ .

fibers<sup>21,22</sup>. Conversely, there is conflicting evidence concerning whether the slow-contracting fibers are affected by  $\beta_2$ -AR agonist treatment in intact animals<sup>23</sup>. In addition, when mice were challenged with specific behavioral tests to evaluate skeletal muscle function, we found an increase of muscle strength in CL316,243-treated mice compared to vehicle-treated animals. Such positive effect was confirmed by the grip strength test, which allowed us to evaluate the peak resistance force, and by the weights test, evaluating the maximal isometric strength.

Several agents have been shown to increase skeletal muscle mass and force<sup>24</sup> by regulating protein synthesis, including anabolic steroids, growth hormones, IGF and  $\beta_2$ -AR agonists<sup>4,25–28</sup>. Most of these factors control the rate of protein turnover at the level of transcription, translation, degradation or a combination of these<sup>29</sup>. According to our previous studies *in vitro*,  $\beta_3$ -ARs stimulation up-regulates protein synthesis and this effect is likely due to the activation of components of the translational machinery, including the ribosomal protein S6<sup>12</sup>. Here, the use of an *in vivo* model confirmed our previous *in vitro* data, thus providing a further demonstration that CL316,243 has the potential to regulate protein metabolism in skeletal muscle by increasing the expression of mTOR targets in the long term. The importance of mTOR in muscle size regulation has been demonstrated by both pharmacological and genetic studies<sup>30–32</sup>. For example, inhibition of mTOR by rapamycin prevented the hypertrophy of myotubes induced *in vitro* by IGF as well as the skeletal muscle hypertrophy *in vivo* induced by overload or clenbuterol<sup>25,33–35</sup>. A decrease in muscle mass and fiber CSA has also been revealed in mTOR and p70<sup>S6K</sup> knockout mice<sup>36,37</sup>. According to Navegantes and collaborators<sup>38</sup>, the anabolic effects of CL316,243 in skeletal muscles are in part due to an inhibition of muscle proteolysis. Such anti-proteolytic effect was particularly evident in rat soleus, but not in extensor digitorum longus, suggesting a different response to  $\beta_3$ -ARs agonist of slow-twitch and fast-twitch muscle. However, the effects of  $\beta_3$ -AR activation in slow-twitch muscle fibers are quite complex since they can also involve the regulation of mitochondrial uncoupling proteins. In particular, immunohistochemical studies have revealed an increase of UCP-3 signals in slow-twitch muscles of obese mice following a chronic administration of CL316,243, which may contribute to the thermogenic effect of  $\beta_3$ -AR agonists<sup>11,39</sup>. In this study, we have also shown that CL316,243 treatment was associated with an increased expression of the nNOS protein in both fast- and slow-twitch muscles. In skeletal muscle, NO has been identified as a physiological intracellular messenger modulating the contractile activity of skeletal muscle, blood flow, exercise-induced skeletal muscle hypertrophy and glucose homeostasis<sup>40–44</sup>. The precise role of the nNOS isoform in skeletal muscle is still a matter of debate, although several lines of evidence suggested that NO plays a key role in the hypertrophic response of skeletal muscle to mechanical and metabolic stimulations<sup>45,46</sup>. NOS activity has been shown to promote transcription of contractile proteins, such as skeletal  $\alpha$ -actin and type I myosin heavy chain mRNA, during chronic skeletal muscle overload<sup>44</sup>. According to our previous studies *in vitro*<sup>47</sup>, the anabolic

effect of NOS might be mediated by the mTOR/p70<sup>S6K</sup> signaling pathway since NOS inhibition by L-NAME prevented the activation of p70<sup>S6K</sup> in response to glucose deprivation. The importance of nNOS in skeletal muscle has been clearly revealed by studies carried out in nNOS-deficient (NOS1<sup>-/-</sup>) mice<sup>48</sup>. These mice presented a significant reduction of muscle mass and CSA of tibialis anterior accompanied by a decrease of muscle force and decreased resistance to fatigue, compared with control mice. Interestingly, the TA of NOS1<sup>-/-</sup> mice showed also lower levels of phosphorylated rpS6, 4E-BP1, and Akt than controls, suggesting that the AKT/mTOR pathway activation was reduced in absence of nNOS. In addition, recent studies have demonstrated that restoration of NO signaling by nNOS overexpression can reduce muscle pathology in mouse models of muscular dystrophy (named mdx mice) by preventing muscle membrane injury and promoting regeneration<sup>49</sup>. A novel important finding of this study is that the acute treatment with CL316,243 induced a significant decrease of the transversal stiffness of single muscle fibers within the first 1000 nm of the fiber surface. This suggests that  $\beta$ 3-AR activation may modulate the elastic properties of near-membrane components, such as the external basal membrane, sarcolemma, cytoskeletal network, and cytoplasm<sup>50</sup>. Further studies are still necessary to clarify the mechanisms by which CL316,243 lowers muscle stiffness and its potential role under pathological conditions associated with high muscle stiffness, including muscle dystrophies. Interestingly,  $\beta$ -adrenergic stimulation has been demonstrated to have also an acute effect on the myocardial stiffness of rabbits<sup>51</sup>. In particular, it has been found that exposure to isoprenaline, a non-selective  $\beta$ -AR agonist, induced a concentration-dependent reduction of myocardial stiffness in papillary muscles isolated from the rabbit's ventricle. In this case, titin phosphorylation was hypothesized as the molecular mechanism responsible for the observed change in stiffness.

Together, these results suggest that targeting  $\beta$ 3-AR may be an effective therapeutic strategy for enhancing muscle growth and strength in a variety of disorders associated with muscle loss and degeneration.

## Methods

**Animals and treatment with CL316,243.** C57Bl/6J wild type male mice aged 3 months were obtained from a breeding colony kept at the University of Naples and University of Catania. Mice were maintained at a controlled temperature ( $21\text{ }^{\circ}\text{C} \pm 1\text{ }^{\circ}\text{C}$ ) and humidity (50%) on a 12 h light/dark cycle (light from 06:00 to 18:00), with ad libitum food and water. All animal experimentation was conducted in accordance with the guidelines laid down by the European Community Council (2010/63/EU). The experimental protocols have been approved by the University Institutional Animal Care and Use Committee from the University of Naples (#0016945, 02/16/2012). Experiments were performed in parallel using 2 groups of mice treated with vehicle ( $n=9$ ) or CL316,243 ( $n=10$ ) at a concentration of 1 mg/kg in saline by subcutaneous injections for 15 days. Two hours after the last injection, mice underwent behavioral assessment of muscular strength by weights test<sup>52</sup> and grip strength test<sup>53</sup>. Mice were then sacrificed by cervical dislocation and muscles were removed and frozen for western blot or processed for CSA evaluation.

**Behavioral assessment of muscle strength.** The weights test was performed as previously described<sup>52</sup>. We used a series of chain links of different weight (from 14 to 74 gr) attached to a ball of fine wire mesh. Each mouse was held by the tail and was allowed to grasp a series of increasing weight steel chain links placed on the laboratory bench. Based on the number of chain links that the mouse was able to grasp and hold for at least 3 seconds, a specific score was assigned. If the mouse dropped the weight in less than 3 sec, the trial was repeated for 3 times and the maximum time/weight achieved was considered for the final scoring. After a rest period of about 20 sec, the next heaviest weight was tested until the mouse failed for 3 consecutive trials. A final total score was calculated as the product of the number of links in the heaviest chain held for the full 3 sec, multiplied by the time (sec) it was held. If the heaviest weight was dropped before 3 sec an appropriate intermediate value was calculated. For example, a mouse holding a 5-link weight for 3 seconds, but unable to lift a 6-link weight, was assigned a score of  $(5 \times 3) = 15$ . If it held the 6-link weight for 1 second, the score was  $(5 \times 3) + (1) = 16$ .

Grip strength test was performed as previously described<sup>53</sup> by using an apparatus equipped with a mouse horizontal forelimb bar (Bioseb, Model GT3). Mice were held by the tail and were allowed to grasp the horizontal bar with the forelimb paws. The mice were then gently pulled backward until they released the grid. The peak force applied by the forelimbs of the mouse was recorded in Newton (N). Each mouse received 3 test trials (with a rest of 2 minutes) for two consecutive sessions (1 hour apart).

**Preparation and Culture of Muscle Fibers.** Untreated adult mice (2–3 months old) were sacrificed by cervical dislocation and FDB muscles were quickly dissected and placed in a small petri dish filled with Tyrode Solution (in mM: 140 NaCl, 2 KCl, 2 CaCl<sub>2</sub>, 10 HEPES, and 5 glucose). FDB muscles were exposed to enzymatic digestion by using 0.2–0.3% Collagenase type I in Tyrode solution for 1 hour at 4 °C and then incubated in 5% CO<sub>2</sub> for 1 hour at 37 °C. After three washes in Tyrode solution containing 10% FBS to block the collagenase effect and stabilize the fibers, FDB muscles were gently triturated to dissociate individual muscle fibers. The fibers were finally plated on laminin-coated culture dishes in serum-containing Tyrode solution and incubated in 5% CO<sub>2</sub> at 37 °C until use.

**Immunofluorescence.** For double immunofluorescence microscopy, the skeletal fibers in culture were fixed in 4% formaldehyde in PBS and permeabilized with PBS-Triton-X100 for 10 min at room temperature. Samples were then incubated for 4 hours with primary antibody against sarcomeric  $\alpha$ -actinin (Sigma A-7811) in order to visualize Z-band on myofilaments. After washing in PBS, fibers were incubated for 1 hour in PBS 1% BSA with TRITC-conjugated goat anti-mouse (AlexaFluor 546). We used FITC-conjugated phalloidin (Sigma-Aldrich; St. Louis) to stain filamentous actin (F-actin) and 4'-6-diamidino-2-phenylindol (DAPI) for nuclei labeling. The specimens were visualized, with an Olympus IX-70 epifluorescence microscope equipped with a Hamamatsu-Orca ER II camera. Image ProPlus was used for the image acquisition.

**Atomic force microscopy.** A commercial atomic force microscope (Keysight Technologies AFM model 5500) mounted on an inverted optical microscope (Olympus IX70) was used to assess the transversal stiffness of single dissociated skeletal muscle fibers<sup>17,54</sup>. Silicon cantilevers with a nominal spring constant  $k = 0.03$  N/m and conical tips (CSC21, MikroMasch, Germany) were used. The spring constant of each cantilever was determined by a thermal noise based method, which ensures a level of accuracy of 10%–15%<sup>55</sup>. To probe the mechanical stiffness onto and below the sarcolemma, we performed force versus distance measurements and evaluated the contact region of the obtained curves. The transversal stiffness was measured as the Young's modulus calculated by considering an approximate purely elastic response of the indented fiber, as proposed by Oliver and collaborators<sup>56</sup>. The stiffness was calculated at different penetration depths by applying controlled forces in the 0.5–2 nN range. Each measurement consisted of 256 force versus distance curves taken on the same  $3 \times 3 \mu\text{m}^2$  region. At least three measurements were performed on a single fiber for each time point (3 and 12 hours) and at least three different fibers were probed for each treated or control condition.

**Histology.** Vehicle and CL316,243-treated mice were sacrificed by cervical dislocation and the limb muscles, TA and soleus, were harvested. Muscles were cross-cut, fixed in 10% buffered formalin, embedded in paraffin, then cut into  $6 \mu\text{m}$ -thick serial sections and mounted on polylysine coated slides. Sections were stained with Hematoxylin and Eosin staining kit (Bio-optica, Milan, Italy), according to manufacturer protocol. Microscopic observation was performed by Leica DM2000LED (Leica Microsystems, Wetzlar, Germany) light microscope equipped with Leica ICC50HD digital camera for photodocumentation. Digital images acquired were then analyzed with SigmaScan Pro 5.0 software (SYSTAT, San Jose, CA, USA) to measure CSA. Measurements were performed by three independent observers and expressed as mean surface area ( $\mu\text{m}^2$ ). A total of 300–350 muscle fibers were analyzed for each muscle.

**Western blot analysis.** TA and soleus of both vehicle and CL316,243-treated mice ( $n = 5$  for each condition) were homogenized in lysis buffer (1:2, w/v) solution containing 0.5 M  $\beta$ -glycerophosphate, 20 mM MgCl<sub>2</sub>, 10 mM ethylene glycol tetraacetic acid, and supplemented with 100 mM dithiothreitol and protease/phosphatase inhibitors (100 mM dimethylsulphonyl fluoride, 2 mg/ml apronitin, 2 mM leupeptin, and 10 mM Na<sub>3</sub>VO<sub>4</sub>). Protein concentration was determined by the Bio-Rad protein assay (Bio-Rad, Milan, Italy). Samples containing 100  $\mu\text{g}$  of proteins were denatured, separated on a 10% (for p70S6K and rpS6) or 8% (for nNOS) SDS-polyacrylamide gel, and electro-transferred onto a nitrocellulose membrane using a Bio-Rad Trans-Blot (Bio-Rad, Italy). Western blotting detection reagents were obtained from Amersham Biosciences (UK); the nitrocellulose membrane was from Hybond ECL (GE Healthcare, UK). Proteins were visualized by reversible staining with Ponceau S solution and destained in PBS<sup>57</sup>. Membranes were blocked at room temperature in milk buffer (1X PBS, 5–10% v/v non-fat dry milk, 0.2% v/v Tween-20) and then incubated at 4 °C overnight with the following primary antibodies: anti-phospho-p70<sup>S6K</sup> (1:1000; Cell Signaling Technology, Massachusetts, USA), anti-phospho-rpS6 (1:1000; Cell Signaling Technology, Massachusetts, USA), anti-nNOS (1:300; Santa Cruz, California, USA); anti- $\alpha$ -tubulin antibody (1:1000; Cell Signaling Technology, Massachusetts, USA) or anti-GAPDH (1:8000; Sigma Aldrich, Milan, Italy). The membranes were then incubated for 90 min at room temperature with 1:5000 horseradish peroxidase-conjugated secondary anti-rabbit or anti-mouse antibodies. The resulting complexes were visualized using chemiluminescence Western blotting detection reagents. The western blot images were scanned using GS-800 imaging densitometer (Bio-Rad, Italy) and analyzed using Quantity One software (Biorad, Italy). The background-subtracted density of the bands in all blots was measured and normalized using  $\alpha$ -tubulin or GAPDH.

**Statistical analysis.** Data are presented as mean  $\pm$  standard error of the mean (SEM). Statistical analyses were performed by using Systat software (Chicago, IL, USA). To compare the experimental conditions, we used unpaired Student's t-test. A single TA and soleus muscle were examined for each treated animal. Two-way ANOVA was used for the AFM data. The level of significance was set at  $p < 0.05$ .

## References

- Kim, Y. S. & Sainz, R. D. Beta-adrenergic agonists and hypertrophy of skeletal muscles. *Life sciences* **50**, 397–407 (1992).
- Lynch, G. S. & Ryall, J. G. Role of beta-adrenoceptor signaling in skeletal muscle: implications for muscle wasting and disease. *Physiological reviews* **88**, 729–767, doi: 10.1152/physrev.00028.2007 (2008).
- Ryall, J. G., Gregorevic, P., Plant, D. R., Sillence, M. N. & Lynch, G. S. Beta 2-agonist fenoterol has greater effects on contractile function of rat skeletal muscles than clenbuterol. *Am J Physiol Regul Integr Comp Physiol* **283**, R1386–R1394, doi: 10.1152/ajpregu.00324.2002 (2002).
- Ryall, J. G., Sillence, M. N. & Lynch, G. S. Systemic administration of beta2-adrenoceptor agonists, formoterol and salmeterol, elicit skeletal muscle hypertrophy in rats at micromolar doses. *British journal of pharmacology* **147**, 587–595, doi: 10.1038/sj.bjp.0706669 (2006).
- Maltin, C. A., Hay, S. M., Delday, M. I., Lobley, G. E. & Reeds, P. J. The action of the beta-agonist clenbuterol on protein metabolism in innervated and denervated phasic muscles. *The Biochemical journal* **261**, 965–971, doi: 10.1042/bj2610965 (1989).
- Zeman, R. J., Peng, H., Danon, M. J. & Etlinger, J. D. Clenbuterol reduces degeneration of exercised or aged dystrophic (mdx) muscle. *Muscle & nerve* **23**, 521–528, doi: 10.1002/(SICI)1097-4598(200004)23:4<521::AID-MUS10>3.0.CO;2-8 (2000).
- Beitzel, F. *et al.* Beta2-adrenoceptor agonist fenoterol enhances functional repair of regenerating rat skeletal muscle after injury. *J Appl Physiol* (1985) **96**, 1385–1392, doi: 10.1152/japplphysiol.01081.2003 (2004).
- Evans, B. A., Papaioannou, M., Bonazzi, V. R. & Summers, R. J. Expression of beta 3-adrenoceptor mRNA in rat tissues. *British journal of pharmacology* **117**, 210–216 (1996).
- Chamberlain, P. D. *et al.* The tissue distribution of the human beta3-adrenoceptor studied using a monoclonal antibody: direct evidence of the beta3-adrenoceptor in human adipose tissue, atrium and skeletal muscle. *Int J Obes Relat Metab Disord* **23**, 1057–1065, doi: 10.1038/sj.ijo.0801039 (1999).

10. Board, M., Doyle, P. & Cawthorne, M. A. BRL37344, but not CGP12177, stimulates fuel oxidation by soleus muscle *in vitro*. *European journal of pharmacology* **406**, 33–34, doi: [http://dx.doi.org/10.1016/S0014-2999\(00\)00671-3](http://dx.doi.org/10.1016/S0014-2999(00)00671-3) (2000).
11. Nakamura, Y. *et al.* Beta 3-adrenergic agonist up-regulates uncoupling proteins 2 and 3 in skeletal muscle of the mouse. *The Journal of veterinary medical science/the Japanese Society of Veterinary Science* **63**, 309–314, doi: <http://doi.org/10.1292/jvms.63.309> (2001).
12. Miniaci, M. C. *et al.* CL316,243, a selective beta3-adrenoceptor agonist, activates protein translation through mTOR/p70S6K signaling pathway in rat skeletal muscle cells. *Pflugers Archiv European journal of physiology* **465**, 509–516, doi: [10.1007/s00424-012-1213-9](https://doi.org/10.1007/s00424-012-1213-9) (2013).
13. Gauthier, C. *et al.* The negative inotropic effect of beta3-adrenoceptor stimulation is mediated by activation of a nitric oxide synthase pathway in human ventricle. *The Journal of clinical investigation* **102**, 1377–1384, doi: [10.1172/JCI2191](https://doi.org/10.1172/JCI2191) (1998).
14. Moniotte, S. *et al.* Upregulation of beta(3)-adrenoceptors and altered contractile response to inotropic amines in human failing myocardium. *Circulation* **103**, 1649–1655, doi: <http://dx.doi.org/10.1161/01.CIR.103.12.1649> (2001).
15. Stamler, J. S. & Meissner, G. Physiology of nitric oxide in skeletal muscle. *Physiological reviews* **81**, 209–237 (2001).
16. Thomas, C. R., Stenson, J. D. & Zhang, Z. Measuring the mechanical properties of single microbial cells. *Adv Biochem Eng Biotechnol* **124**, 83–98, doi: [10.1007/10\\_2010\\_84](https://doi.org/10.1007/10_2010_84) (2011).
17. Khairallah, R. J. *et al.* Microtubules underlie dysfunction in duchenne muscular dystrophy. *Sci Signal* **5**, ra56, doi: [10.1126/scisignal.2002829](https://doi.org/10.1126/scisignal.2002829) (2012).
18. Haase, K. & Pelling, A. E. Investigating cell mechanics with atomic force microscopy. *J R Soc Interface* **12**, 20140970, doi: [10.1098/rsif.2014.0970](https://doi.org/10.1098/rsif.2014.0970) (2015).
19. Brixius, K. *et al.* Beta3-adrenergic eNOS stimulation in left ventricular murine myocardium. *Can J Physiol Pharmacol* **84**, 1051–1060, doi: [10.1139/y06-033](https://doi.org/10.1139/y06-033) (2006).
20. Idigo, W., Zhang, M. H., Zhang, Y. H. & Casadei, B. The negative inotropic effect of [beta]3-adrenergic receptor stimulation in nNOS-/- mice is restored by oxypurinol. *Heart* **92**, e1–008 (2006).
21. Zeman, R. J., Ludemann, R., Easton, T. G. & Etlinger, J. D. Slow to fast alterations in skeletal muscle fibers caused by clenbuterol, a beta 2-receptor agonist. *The American journal of physiology* **254**, E726–E732 (1988).
22. Mounier, R., Cavalie, H., Lac, G. & Clottes, E. Molecular impact of clenbuterol and isometric strength training on rat EDL muscles. *Pflugers Archiv: European journal of physiology* **453**, 497–507, doi: [10.1007/s00424-006-0122-1](https://doi.org/10.1007/s00424-006-0122-1) (2007).
23. Sato, S., Shirato, K., Tachiyashiki, K. & Imaizumi, K. Muscle plasticity and beta(2)-adrenergic receptors: adaptive responses of beta(2)-adrenergic receptor expression to muscle hypertrophy and atrophy. *Journal of biomedicine & biotechnology* **2011**, 729598, doi: [10.1155/2011/729598](https://doi.org/10.1155/2011/729598) (2011).
24. Blaauw, B. *et al.* Inducible activation of Akt increases skeletal muscle mass and force without satellite cell activation. *FASEB journal: official publication of the Federation of American Societies for Experimental Biology* **23**, 3896–3905, doi: [10.1096/fj.09-131870](https://doi.org/10.1096/fj.09-131870) (2009).
25. Bodine, S. C. *et al.* Akt/mTOR pathway is a crucial regulator of skeletal muscle hypertrophy and can prevent muscle atrophy *in vivo*. *Nature cell biology* **3**, 1014–1019, doi: [10.1038/ncb1101-1014](https://doi.org/10.1038/ncb1101-1014) (2001).
26. Monda, M. *et al.* Inhibition of prostaglandin synthesis reduces the induction of MyoD expression in rat soleus muscle. *J Muscle Res Cell Motil* **30**, 139–144, doi: [10.1007/s10974-009-9182-0](https://doi.org/10.1007/s10974-009-9182-0) (2009).
27. Kimball, S. R. & Jefferson, L. S. Control of translation initiation through integration of signals generated by hormones, nutrients, and exercise. *The Journal of biological chemistry* **285**, 29027–29032, doi: [10.1074/jbc.R110.137208](https://doi.org/10.1074/jbc.R110.137208) (2010).
28. Koopman, R. *et al.* Cellular mechanisms underlying temporal changes in skeletal muscle protein synthesis and breakdown during chronic beta-adrenoceptor stimulation in mice. *The Journal of physiology* **588**, 4811–4823, doi: [10.1113/jphysiol.2010.196725](https://doi.org/10.1113/jphysiol.2010.196725) (2010).
29. Schiaffino, S., Dyar, K. A., Ciciliot, S., Blaauw, B. & Sandri, M. Mechanisms regulating skeletal muscle growth and atrophy. *The FEBS journal* **280**, 4294–4314, doi: [10.1111/febs.12253](https://doi.org/10.1111/febs.12253) (2013).
30. Goodman, C. A. *et al.* A phosphatidylinositol 3-kinase/protein kinase B-independent activation of mammalian target of rapamycin signaling is sufficient to induce skeletal muscle hypertrophy. *Molecular biology of the cell* **21**, 3258–3268, doi: [10.1091/mbc.E10-05-0454](https://doi.org/10.1091/mbc.E10-05-0454) (2010).
31. Goodman, C. A. *et al.* The role of skeletal muscle mTOR in the regulation of mechanical load-induced growth. *The Journal of physiology* **589**, 5485–5501, doi: [10.1113/jphysiol.2011.218255](https://doi.org/10.1113/jphysiol.2011.218255) (2011).
32. Mounier, R. *et al.* Antagonistic control of muscle cell size by AMPK and mTORC1. *Cell Cycle* **10**, 2640–2646, doi: [10.4161/cc.10.16.17102](https://doi.org/10.4161/cc.10.16.17102) (2011).
33. Kline, W. O., Panaro, F. J., Yang, H. & Bodine, S. C. Rapamycin inhibits the growth and muscle-sparing effects of clenbuterol. *J Appl Physiol* **102**, 740–747, doi: [10.1152/jappphysiol.00873.2006](https://doi.org/10.1152/jappphysiol.00873.2006) (2007).
34. Rommel, C. *et al.* Mediation of IGF-1-induced skeletal myotube hypertrophy by PI(3)K/Akt/mTOR and PI(3)K/Akt/GSK3 pathways. *Nature cell biology* **3**, 1009–1013, doi: [10.1038/ncb1101-1009](https://doi.org/10.1038/ncb1101-1009) (2001).
35. Bentzinger, C. F. *et al.* Differential response of skeletal muscles to mTORC1 signaling during atrophy and hypertrophy. *Skelet Muscle* **3**, 6, doi: [10.1186/2044-5040-3-6](https://doi.org/10.1186/2044-5040-3-6) (2013).
36. Risso, V. *et al.* Muscle inactivation of mTOR causes metabolic and dystrophin defects leading to severe myopathy. *The Journal of cell biology* **187**, 859–874, doi: [10.1083/jcb.200903131](https://doi.org/10.1083/jcb.200903131) (2009).
37. Ruvinsky, I. *et al.* Mice deficient in ribosomal protein S6 phosphorylation suffer from muscle weakness that reflects a growth defect and energy deficit. *PLoS one* **4**, e5618, doi: [10.1371/journal.pone.0005618](https://doi.org/10.1371/journal.pone.0005618) (2009).
38. Navegantes, L. C., Resano, N. M., Baviera, A. M., Migliorini, R. H. & Kettelhut, I. C. CL 316,243, a selective beta3-adrenergic agonist, inhibits protein breakdown in rat skeletal muscle. *Pflugers Archiv: European journal of physiology* **451**, 617–624, doi: [10.1007/s00424-005-1496-1](https://doi.org/10.1007/s00424-005-1496-1) (2006).
39. Yoshida, T. *et al.* Beta 3-Adrenergic agonist induces a functionally active uncoupling protein in fat and slow-twitch muscle fibers. *The American journal of physiology* **274**, E469–E475 (1998).
40. Kobzik, L., Reid, M. B., Bredt, D. S. & Stamler, J. S. Nitric oxide in skeletal muscle. *Nature* **372**, 546–548, doi: [10.1038/372546a0](https://doi.org/10.1038/372546a0) (1994).
41. Reid, M. B. Role of nitric oxide in skeletal muscle: synthesis, distribution and functional importance. *Acta Physiol Scand* **162**, 401–409, doi: [10.1046/j.1365-201X.1998.0303f.x](https://doi.org/10.1046/j.1365-201X.1998.0303f.x) (1998).
42. Bradley, S. J., Kingwell, B. A. & McConell, G. K. Nitric oxide synthase inhibition reduces leg glucose uptake but not blood flow during dynamic exercise in humans. *Diabetes* **48**, 1815–1821, doi: [10.2337/diabetes.48.9.1815](https://doi.org/10.2337/diabetes.48.9.1815) (1999).
43. Anderson, J. E. A role for nitric oxide in muscle repair: nitric oxide-mediated activation of muscle satellite cells. *Molecular biology of the cell* **11**, 1859–1874 (2000).
44. Suhr, F., Gehlert, S., Grau, M. & Bloch, W. Skeletal muscle function during exercise-fine-tuning of diverse subsystems by nitric oxide. *International journal of molecular sciences* **14**, 7109–7139, doi: [10.3390/ijms14047109](https://doi.org/10.3390/ijms14047109) (2013).
45. Zhang, J. S., Kraus, W. E. & Truskey, G. A. Stretch-induced nitric oxide modulates mechanical properties of skeletal muscle cells. *American journal of physiology. Cell physiology* **287**, C292–C299, doi: [10.1152/ajpcell.00018.2004](https://doi.org/10.1152/ajpcell.00018.2004) (2004).
46. Ito, N., Ruegg, U. T., Kudo, A., Miyagoe-Suzuki, Y. & Takeda, S. Activation of calcium signaling through Trpv1 by nNOS and peroxynitrite as a key trigger of skeletal muscle hypertrophy. *Nature medicine* **19**, 101–106, doi: [10.1038/nm.3019](https://doi.org/10.1038/nm.3019) (2013).
47. Miniaci, M. C. *et al.* Glucose deprivation promotes activation of mTOR signaling pathway and protein synthesis in rat skeletal muscle cells. *Pflugers Archiv: European journal of physiology* **467**, 1357–1366, doi: [10.1007/s00424-014-1583-2](https://doi.org/10.1007/s00424-014-1583-2) (2015).



48. De Palma, C. *et al.* Deficient nitric oxide signalling impairs skeletal muscle growth and performance: involvement of mitochondrial dysregulation. *Skelet Muscle* **4**, 22, doi: 10.1186/s13395-014-0022-6 (2014).
49. Wehling, M., Spencer, M. J. & Tidball, J. G. A nitric oxide synthase transgene ameliorates muscular dystrophy in mdx mice. *The Journal of cell biology* **155**, 123–131, doi: 10.1083/jcb.200105110 (2001).
50. Defranchi, E. *et al.* Imaging and elasticity measurements of the sarcolemma of fully differentiated skeletal muscle fibres. *Microscopy research and technique* **67**, 27–35, doi: 10.1002/jemt.20177 (2005).
51. Falcao-Pires, I., Fontes-Sousa, A. P., Lopes-Conceicao, L., Bras-Silva, C. & Leite-Moreira, A. F. Modulation of myocardial stiffness by beta-adrenergic stimulation—its role in normal and failing heart. *Physiological research/Academia Scientiarum Bohemoslovaca* **60**, 599–609 (2011).
52. Deacon, R. M. Measuring the strength of mice. *Journal of visualized experiments* **76**, e2610, doi: 10.3791/2610 (2013).
53. Nieoczym, D., Socala, K., Jedziniak, P., Olejnik, M. & Wlaz, P. Effect of sildenafil, a selective phosphodiesterase 5 inhibitor, on the anticonvulsant action of some antiepileptic drugs in the mouse 6-Hz psychomotor seizure model. *Progress in neuro-psychopharmacology & biological psychiatry* **47**, 104–110, doi: 10.1016/j.pnpbp.2013.08.009 (2013).
54. Canato, M. *et al.* Mechanical and electrophysiological properties of the sarcolemma of muscle fibers in two murine models of muscle dystrophy: col6a1<sup>-/-</sup> and mdx. *Journal of biomedicine & biotechnology* **2010**, 981945; doi: 10.1155/2010/981945 (2010).
55. Hutter, J. L. & Bechhoefer, J. Calibration of atomic-force microscope tips. *Rev. Sci. Instrum.* **64**, 1868–1873, doi: <http://dx.doi.org/10.1063/1.1143970> (1993).
56. Oliver, W. C. & Pharr, G. M. Measurement of hardness and elastic modulus by instrumented indentation: Advances in understanding and refinements to methodology. *Journal of Materials Research* **19**, 3–20, doi: <http://dx.doi.org/10.1557/jmr.2004.19.1.3> (2004).
57. Miniaci, M. C. *et al.* Cysteine Prevents the Reduction in Keratin Synthesis Induced by Iron Deficiency in Human Keratinocytes. *Journal of cellular biochemistry* **117**, 402–412, doi: 10.1002/jcb.25286 (2016).

## Acknowledgements

We thank Angelo Russo and Giovanni Esposito for their valuable technical assistance. The present research was supported by Bank of Italy grant #744460/13 to Maria Concetta Miniaci. The funding sources had no involvement in the study design, collection, analysis or interpretation of data, in the writing of the report, or in the decision to submit for publication.

## Author Contributions

D.P. and W.G. performed behavioral experiments; C.C. performed cross-sectional area experiments; E.P., R.C. and P.L. performed western blot experiments; M.T. performed isolation, culturing and immunocytochemistry of muscle fibers; R.R. and L.D. performed atomic force microscopy; D.P., R.R., A.P., and P.S. contributed through numerous discussions; M.C.M. and D.P. wrote the paper; P.S. and M.C.M supervised the project.

## Additional Information

**Competing financial interests:** The authors declare no competing financial interests.

**How to cite this article:** Puzzo, D. *et al.* CL316,243, a  $\beta$ 3-adrenergic receptor agonist, induces muscle hypertrophy and increased strength. *Sci. Rep.* **6**, 37504; doi: 10.1038/srep37504 (2016).

**Publisher's note:** Springer Nature remains neutral with regard to jurisdictional claims in published maps and institutional affiliations.



This work is licensed under a Creative Commons Attribution 4.0 International License. The images or other third party material in this article are included in the article's Creative Commons license, unless indicated otherwise in the credit line; if the material is not included under the Creative Commons license, users will need to obtain permission from the license holder to reproduce the material. To view a copy of this license, visit <http://creativecommons.org/licenses/by/4.0/>

© The Author(s) 2016